Relationship between charge stripe order and structural phase transitions in La1.875Ba0.125-xSrxCu04

著者	Kimura H., Noda Y., Goka H., Fujita M., Yamada K., Mizumaki M., Ikeda N., Ohsumi H.
journal or publication title	Physical Review. B
volume	70
number	13
page range	134512
year	2004
URL	http://hdl.handle.net/10097/53577

doi: 10.1103/PhysRevB.70.134512

Relationship between charge stripe order and structural phase transitions in $La_{1.875}Ba_{0.125-x}Sr_xCuO_4$

H. Kimura,[1,*] Y. Noda,[1] H. Goka,[2] M. Fujita,[2] K. Yamada,[2] M. Mizumaki,[3] N. Ikeda,[3] and H. Ohsumi[3]
[1]*Institute of Multidisciplinary Research for Advanced Materials, Tohoku University, Sendai 980-8577, Japan*
[2]*Institute for Materials Research, Tohoku University, Sendai 980-8577, Japan*
[3]*Japan Synchrotron Radiation Research Institute, Hyogo 679-5198, Japan*
(Received 22 February 2004; revised manuscript received 12 August 2004; published 22 October 2004)

The nature of charge stripe order and its relationship with structural phase transitions were studied using synchrotron x-ray diffraction in $La_{1.875}Ba_{0.125-x}Sr_xCuO_4$ ($0.05 \leqslant x \leqslant 0.10$). For $x=0.05$, as temperature increased, incommensurate superlattice peaks associated with the charge order disappeared just at the structural phase transition temperature, T_{d2}. However, for $x=0.075$ and 0.09, the superlattice peaks still existed as a short range correlation even above T_{d2}, indicating a precursor of charge ordering. Furthermore, temperature dependences of the superlattice peak intensity, correlation length, and incommensurability for $x=0.05$ are different from those for $x=0.075$ and 0.09. These results suggest that the transition process into the charge stripe order strongly correlates with the order of the structural phase transitions. A quantitative comparison of the structure factor associated with the charge order have been also made for all the samples.

DOI: 10.1103/PhysRevB.70.134512 PACS number(s): 74.72.Dn, 71.45.Lr, 61.10.−i

I. INTRODUCTION

For the past several years, the relationship between charge stripe correlations[1] and high- T_c superconductivity has been intensively studied to clarify whether the role of the stripes for the superconductivity is positive or negative. Systematic studies on the $La_{1.6-x}Nd_{0.4}Sr_xCuO_4$ (LNSCO) system have shown that for the low-temperature tetragonal (LTT; $P4_2/ncm$) phase, incommensurate (IC) charge and magnetic orders are stabilized and compete with superconductivity.[2–4] This result provided a qualitative explanation for the long-standing mystery of the "1/8-problem" in La-214 cuprates,[5,6] namely, the *ordered state* of charge stripes induced by the LTT transformation has a negative impact with high-T_c superconductivity.

In the 1/8-hole-doped $La_{1.875}Ba_{0.125-x}Sr_xCuO_4$ (LBSCO) system, the crystal structure at the lowest temperature changes from LTT to a low-temperature-orthorhombic (LTO; *Bmab*) phase via the low-temperature-less-orthorhombic (LTLO; *Pccn*) phase, as Sr-concentration x increases (see Fig. 1). Fujita *et al.* have composed a detailed phase diagram of the crystal structure, IC charge/magnetic order, and T_c for this system,[7] where the charge order is stabilized only in LTT and LTLO phases (gray-hatched region in Fig. 1) and competes with superconductivity. On the contrary, the magnetic order in this system, which is robust in all the structural phases, shows a weak competition with the superconductivity.

The momentum structure and the temperature evolution of the charge order in the LBSCO system have been studied by neutron diffraction[8] as well as x-ray diffraction.[9] In the LTT phase for $x=0.05$, the IC modulation wave vector ($\equiv q_{\rm ch}$) of the charge order is $(2\varepsilon,0,1/2)$ with high-temperature-tetragonal (HTT; $I4/mmm$) notation. However in the LTLO phase for $x=0.075$, $q_{\rm ch}$ shifts away from the tetragonal-symmetric position to an orthorhombic-symmetric position, giving the wave vector of $(+2\varepsilon,-2\eta,1/2)$. The charge order in this system is stabilized just below the temperature where the structural phase transition from LTO into LTT or LTLO phase occurs ($\equiv T_{d2}$). Further, the ordered state evolves as the order parameter of the LTT or LTLO structure increases. These facts clearly show that a strong correlation exists between the charge order and the crystal structure, giving rise to suppression of superconductivity.

The charge order is detectable as lattice distortions in neutron and x-ray diffraction measurements. Recently, our preliminary x-ray diffraction measurements showed that the IC superlattice peaks at $(6+2\varepsilon,0,11/2)$ are ~10 times stronger in intensity than that at $(2+2\varepsilon,0,1/2)$. This is due to the amplitude of the scattering wave vector $|Q|$ and the strong L

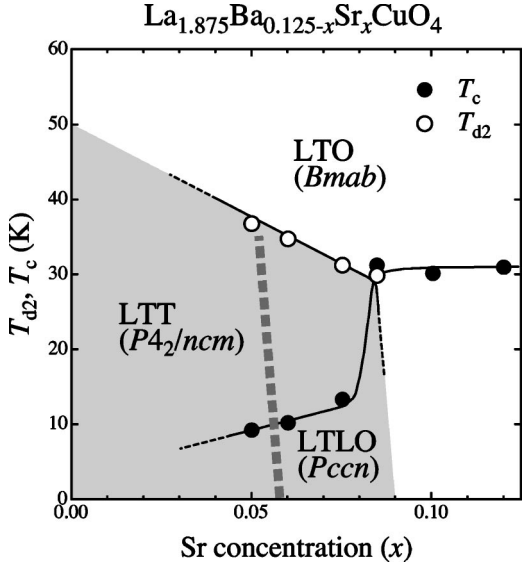

FIG. 1. Structural phase transition temperature T_{d2} and superconducting transition temperature T_c as a function of Sr concentration for the $La_{1.875}Ba_{0.125-x}Sr_xCuO_4$ system, after Fujita *et al.* (Ref. 7).

dependence of the structure factor for the superlattice peak,[10] suggesting the importance of lattice distortions along the c axis. This result indicates that the superlattice peak at higher-Q positions is much more sensitive to the charge order (or the lattice distortion) than that at lower-Q positions observed previously.[9,11] This motivated us to conduct detailed measurements of IC superlattice peaks at higher-Q position, especially at $(6+2\varepsilon,0,11/2)$ or $(6-2\varepsilon,0,17/2)$, for $La_{1.875}Ba_{0.125-x}Sr_xCuO_4$ using a synchrotron x-ray source for diffraction studies, which can elucidate detailed differences between the nature of charge stripes in the LTT and LTLO phases. In this paper, we show that for $x=0.075$ and $x=0.09$, short-range charge correlation starts appearing even above T_{d2} while the correlations appear just at T_{d2} for $x=0.05$. The results imply that the evolution of the charge stripes in the LTLO phase is different from that in the LTT phase, which relates to the order of the structural phase transition from the LTO to the LTT or LTLO phase. We also show the possibility that the displacement pattern of the atoms induced by the charge stripe order in the LTT phase is different from that in the LTLO phase.

II. EXPERIMENT

Single crystals of LBSCO with $x=0.05$, 0.075, 0.09, and 0.10 were cut into a cylindrical shape with dimensions of 0.43 mm diameter and 5 mm height, where the longest axis was parallel to the c axis. X-ray diffraction experiments were performed at the Beam-line BL46XU and BL02B1[12] of Japan Synchrotron Radiation Research Institute in SPring-8. The x-ray energy was tuned to 20 keV and 32.6 keV using a Si(111) double monochromator at BL46XU and BL02B1, respectively. A double platinum mirror was inserted to eliminate higher order harmonics of the x rays. The samples were cooled down to 7 K using a closed-cycled ^{4}He refrigerator. In this paper, the reciprocal lattice is defined in the $I4/mmm$ symmetry where the two short axes correspond to the distance between the nearest-neighbor Cu atoms along the in-plane Cu-O bond. Typical instrument resolutions along the H and K directions were 0.0039 Å^{-1} and 0.0037 Å^{-1} at $Q=(6,0,6)$, and 0.0038 Å^{-1} and 0.0016 Å^{-1} at $Q=(4,0,0)$, respectively. In the present study, we obtained nearly single-domain orthorhombic crystals for $x=0.075$, 0.09, and 0.10. Note that the measurements for $x=0.05$ and 0.075 were done at BL46XU and those for $x=0.09$ and 0.10 were carried out at BL02B1.

As mentioned in Sec. I, we focused on the measurements of the superlattice peaks at $Q_{ch}=(h\pm2\varepsilon,0,l/2)$ with $h=6,8$ and $l=11,17$ in the present study. $(5,0,0)$ and $(7,0,0)$ Bragg reflections, which appears only in the LTT and LTLO phases and corresponds to the order parameter for these phases, were also measured to compare the phase transition of the charge order with that of the crystal structure. Note that we obtained a much better signal-to-noise ratio than that in the previous study[9] by measuring the superlattice peaks at $L=11/2,17/2$. Thus in this paper, we show q profiles as a raw data, not as a subtracted data.

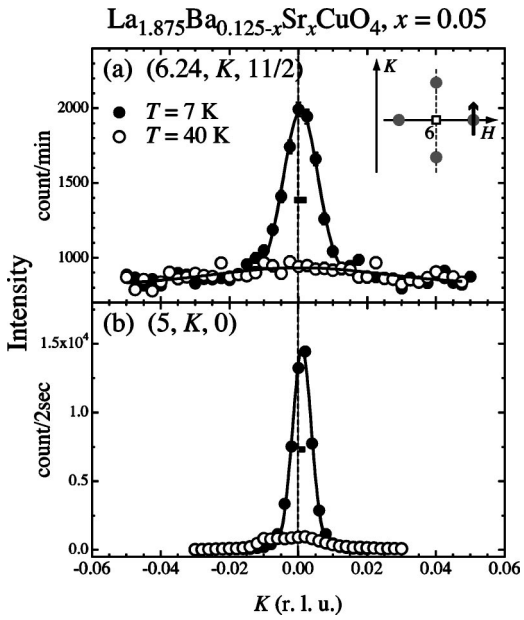

FIG. 2. q profiles along the K direction of (a) superlattice peak through $Q_{ch}=(6.24,0,11/2)$, (b) $(5,0,0)$ Bragg reflection for $x=0.05$. Scan trajectory and confirmed peak positions of superlattice peaks are illustrated in the inset of (a). Closed and open circles correspond to the data taken at 7 K and 40 K, respectively. Bold horizontal lines correspond to the instrument resolutions.

III. RESULTS

A. Q dependence

Q-scan profiles along the K direction of the superlattice peak and the $(5,0,0)$ peak for $x=0.05$, taken at $T=7$ K and 40 K, are shown in Fig. 2. The trajectory of the q scan for the superlattice peak is shown in the inset of Fig. 2(a). H and K scans for the superlattice peak at $T=7$ K confirmed that a quartet of superlattice peaks are located exactly at $Q_{ch}=(6\pm2\varepsilon,0,L/2)$, $(6,\pm2\varepsilon,L/2)$ with $2\varepsilon=0.2390(5)$ r.l.u., for which the geometry is consistent with the crystal symmetry of the LTT structure.

The observed linewidth along the K direction for the superlattice peak is apparently broader than the instrument resolution (denoted in the figure as a bold horizontal line), giving a finite correlation length for the charge correlations. Note that the linewidth along the H direction for the superlattice peaks becomes also broader.

As a result, the correlation lengths of the charge order along the a and b axis $[\equiv\xi_{ch}(a),\xi_{ch}(b)]$ are 98 ± 4 Å and 110 ± 4 Å at $T=7$ K, respectively. For the $(5,0,0)$ peak, the linewidth along the K direction is broader than the instrumental resolution while the linewidth along the H direction reaches the resolution limit. Thus the correlation length for the LTT structure, ξ_a and ξ_b, are estimated to be >300 Å and 196 ± 5 Å, respectively, indicating a large anisotropy of the structural coherence or a mosaic spread due to a local disorder at the LTT phase. At $T=40$ K, just below T_{d2}, both the superlattice peak and the $(5,0,0)$ peak almost vanish, indicating that the charge order appears when the structural phase transition into the LTT phase occurs.

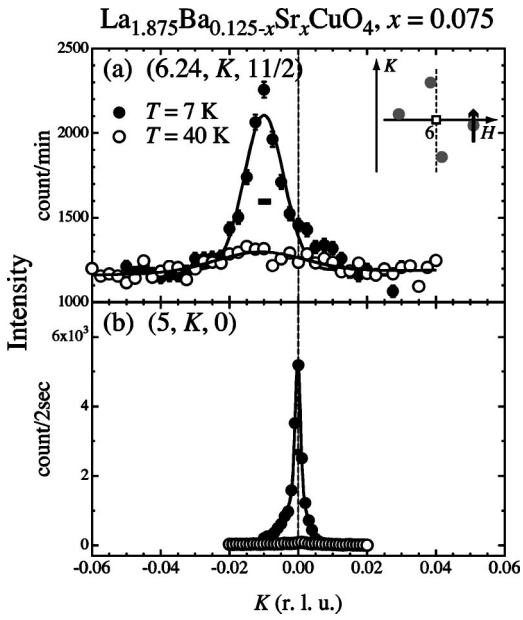

FIG. 3. q profiles along the K direction of (a) superlattice peak through $Q_{\mathrm{ch}}=(6.24,-0.01,11/2)$, (b) $(5,0,0)$ Bragg reflection for $x=0.075$. Scan trajectory and confirmed peak positions of superlattice peaks are illustrated in the inset of (a). Closed and open circles correspond to the data taken at 7 K and 40 K, respectively. Bold horizontal lines correspond to the instrument resolutions.

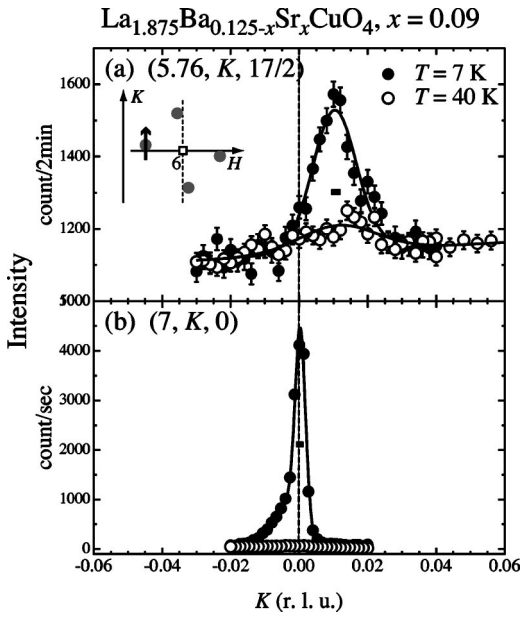

FIG. 4. q profiles along the K direction of (a) superlattice peak through $Q_{\mathrm{ch}}=(5.76,0.01,17/2)$, (b) $(7,0,0)$ Bragg reflection for $x=0.09$. Scan trajectory and confirmed peak positions of superlattice peaks are illustrated in the inset of (a). Closed and open circles correspond to the data taken at 7 K and 40 K, respectively. Bold horizontal lines correspond to the instrument resolutions.

Figures 3(a) and 3(b) show q-scan profiles along the K direction of the superlattice peak and the $(5,0,0)$ peak for $x=0.075$, respectively, also taken at $T=7$ K and 40 K. The trajectory of the q scan for the superlattice peak is displayed in the inset of Fig. 3(a). Since the single-domain-LTLO phase was obtained for the $x=0.075$ sample, we confirmed that a shift of the superlattice peaks from the highly symmetric axis clearly exists and the exact peak position is determined as $Q_{\mathrm{ch}}=(6\pm 2\varepsilon, \mp 2\eta, L/2)$, $(6\mp 2\eta, \pm 2\varepsilon, L/2)$ with $2\varepsilon=0.2360(5)$ r.l.u. and $2\eta=0.0100(5)$ r.l.u. The observed linewidth along the K direction for the superlattice peak is much broader than the resolution, of which value is almost comparable to that for $x=0.05$. On the other hand, the linewidth for the $(5,0,0)$ peak is resolution limited, which is much sharper than that for $x=0.05$. Therefore, $\xi_{\mathrm{ch}}(a)$ and $\xi_{\mathrm{ch}}(b)$ for the charge order are 104 ± 5 Å and 100 ± 7 Å, respectively, while ξ_a and ξ_b for the LTLO structural coherence become long ranged, which is in contrast with the results for $x=0.05$. At $T=40$ K, far above T_{d2}, the broad superlattice peak clearly remains while the $(5,0,0)$ peak disappears, suggesting that the charge order exists even above T_{d2} with a short range correlation.

Figures 4(a) and 4(b) show q-scan profiles at $T=7$ K and 40 K along the K direction of the superlattice peak through $(5.76,0.01,17/2)$ and the $(7,0,0)$ peak for $x=0.09$, respectively, taken at BL02B1. The trajectory of the q-scan for the superlattice peak is displayed in the inset of Fig. 4(a). This sample also had the single domained structure at LTLO phase. Thus the exact values of 2ε and 2η are obtained as 0.2403(5) and 0.0103(3), respectively. As seen in Fig. 4(a), the linewidth along the K direction is much broader than the resolution, which is also seen in the linewidth along H. As a result, $\xi_{\mathrm{ch}}(a)$ and $\xi_{\mathrm{ch}}(b)$ for the charge order become 80 ± 4 Å and 80 ± 5 Å, respectively, which is shorter than those for $x=0.05$ and $x=0.075$. As for the $(7,0,0)$ peak, the linewidth is somewhat broader than the resolution but ξ_a and ξ_b still extend over 200 Å. Although the $(5,0,0)$ peak completely disappears at $T=40$ K, the broad superlattice peak still clearly exists, which is consistent with the results of $x=0.075$. We had observed no superlattice peak in the $x=0.10$ sample but observed quite weak (5, 0, 0) peak, indicating that the development of the order parameter for the LTLO phase is too small to stabilize the charge order.

In our previous paper, we argued for the anisotropy of $\xi_{\mathrm{ch}}(a)$ and $\xi_{\mathrm{ch}}(b)$, based on the comparison with the ξ_a and ξ_b of LTT/LTLO structure.[9] However, the present study, under the fine resolution in q space, has shown that the structural coherence for the LTT phase is apparently different from that for the LTLO phase, which was not observed in the previous experiment. Therefore in the present study, we evaluated the value of $\xi_{\mathrm{ch}}(a)$ and $\xi_{\mathrm{ch}}(b)$ by comparing the observed linewidths of fundamental Bragg peaks taken at room temperature, which corresponds to the accurate instrument resolutions.

B. *T* dependence

The temperature dependence of integrated intensity, linewidth, 2ε, and 2η were measured in detail for the IC superlattice peaks for $x=0.05$, $x=0.075$, and $x=0.09$. For the $(5,0,0)$ and $(7,0,0)$ peak, the temperature dependence of integrated intensity and linewidth were measured. All the measurements were performed during heating process.

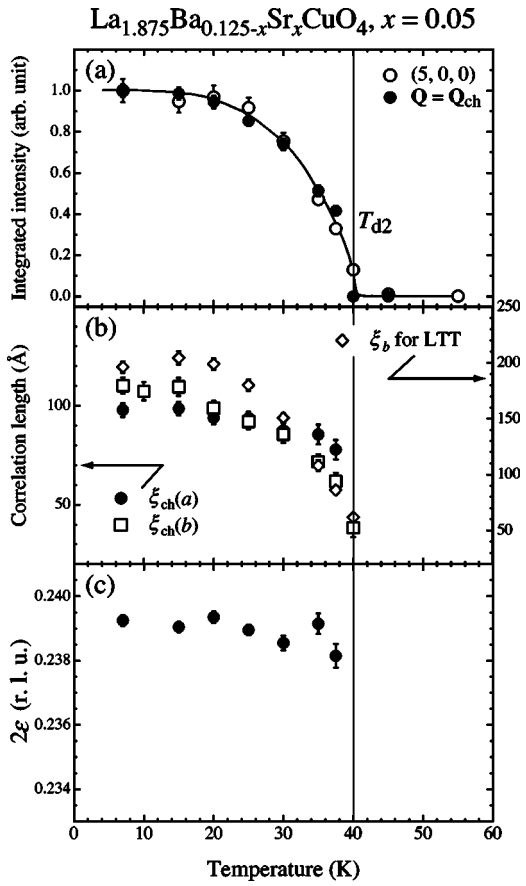

FIG. 5. Temperature dependences of (a) integrated intensity for the superlattice peak (closed circles) and the (5,0,0) peak (open circles), (b) correlation length along the *a* axis (closed circles), *b* axis (open squares), (c) 2ε for $x=0.05$. The correlation length along *b* axis for LTT structure is plotted in (b) with open diamonds against a right vertical axis. The solid curve in (a) is to guide the eye.

The results for $x=0.05$ are summarized in Fig. 5. Figure 5(a) shows the temperature dependence of integrated intensity for the superlattice peak at $Q_{\mathrm{ch}}=(6.239,0,11/2)$ and the $(5,0,0)$ peak, where the intensities are normalized at 7 K. It is seen that the evolution of the intensity for the superlattice peak agrees well with that for the $(5,0,0)$ peak, apparently indicating that the charge order appears just at T_{d2} ($\sim$40 K) and the order parameters for the charge order and the LTT structure are strongly associated with each other. $\xi_{\mathrm{ch}}(a)$ and $\xi_{\mathrm{ch}}(b)$ for the charge order and ξ_b for the LTT structure as a function of temperature are plotted in Fig. 5(b), for which values are obtained from the inverse of the intrinsic linewidth. Note that ξ_a for the LTT phase cannot be plotted in the figure because the correlation along the *a* axis becomes almost a long-range one below T_{d2}. As temperature decreases, both $\xi_{\mathrm{ch}}(a)$ and $\xi_{\mathrm{ch}}(b)$ increase and show a nearly isotropic correlation with the length of $\sim$100 Å. In the case of $\xi_{\mathrm{ch}}(b)$, the temperature variation is quite similar to the development of ξ_b for the LTT structure, implying that the growth of the charge correlation follows the evolution of the LTT structural coherence along the *b* axis. As seen in Fig. 5(c), the incommensurability 2ε for $x=0.05$ is nearly constant for all temperature regions below T_{d2}.

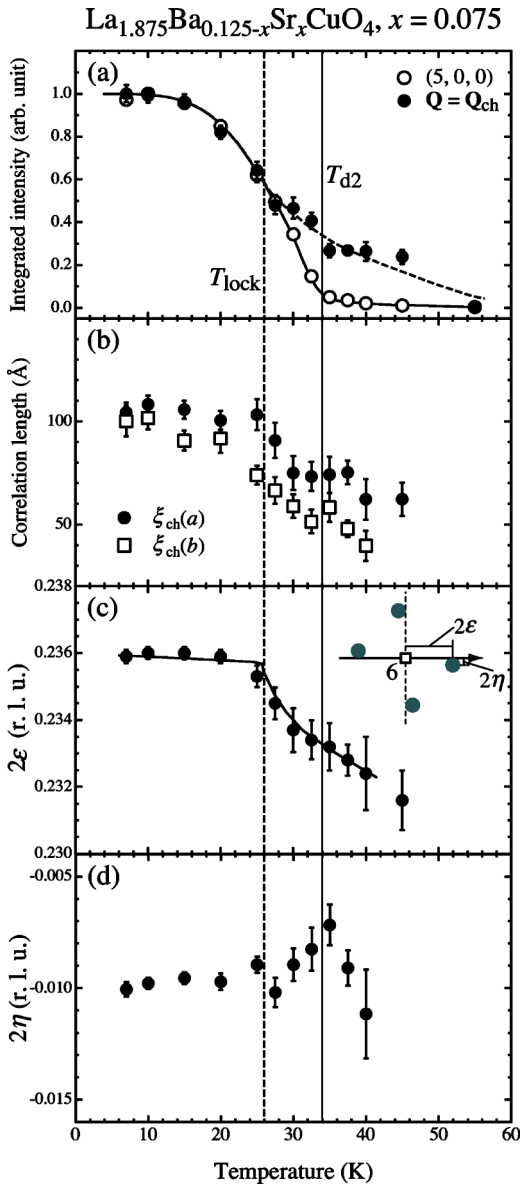

FIG. 6. Temperature dependences of (a) integrated intensity for the superlattice peak (closed circles) and the (5,0,0) peak (open circles), (b) correlation length along the *a* axis (closed circles) and *b* axis (open squares), (c) 2ε, (d) 2η for $x=0.075$. Definitions of 2ε and 2η are shown in the inset of (c). The bold and dashed curves are guides to the eye.

Figure 6 shows the summary of results for $x=0.075$.

The integrated intensity of the superlattice peak and the $(5,0,0)$ peak are depicted in Fig. 6(a) as a function of temperature. The $(5,0,0)$ peak starts growing below T_{d2} ($\sim$34 K) where the structural phase transition from the LTO to the LTLO phase occurs, while the superlattice peak appears at a much higher temperature than T_{d2}. In the lower temperature region, the temperature dependence of the superlattice peak intensity coincides with that for the $(5,0,0)$ peak intensity, which is also seen in the results for $x=0.05$. However, above $T\sim 26$ K (indicated in Fig. 6 as a vertical dashed line), the superlattice peak intensity decreases more gradually than the decay of the $(5,0,0)$ peak with increasing tem-

perature. The temperature dependence of the correlation length for the charge order is plotted in Fig. 6(b). Both ξ_a and ξ_b for LTLO structural coherence are not shown because the correlations along *a* and *b* axis reach at least 300 Å for all temperature regions below T_{d2}. At the lowest temperature, the correlation of the charge order is nearly isotropic with the length of ~100 Å which is almost identical to the charge correlation for $x=0.05$. However, one can see in Fig. 6(b) that the correlation length suddenly changes around $T \sim 26$ K, which is not seen in the charge correlation for $x=0.05$. As shown in Figs. 6(c) and 6(d), the incommensurability 2ε starts increasing with decreasing temperature and saturates below ~26 K while the peak shift 2η from the fundamental axis is almost temperature independent. These results imply that the charge order initially appears as short range correlations well above T_{d2} and the correlation starts extending well below T_{d2}, where the IC modulation vector for the charge order is locked into $2\varepsilon=0.236$ r.l.u. In this paper, we defined the temperature where the $Q_{\rm ch}$ is locked as $T_{\rm lock}$.

The summary of the results for $x=0.09$ is shown in Fig. 7. The temperature dependence of the integrated intensity for the superlattice peak and the (7,0,0) peak are displayed in Fig. 7(a). The intensities are normalized by the values taken at $T=7$ K. As temperature decreases, the structure phase transition into LTLO phase occurs at T_{d2} (~30 K) which follows the appearance of the superlattice peak. Around the lowest temperature, the temperature evolution of the superlattice peak almost coincides with that of the (7,0,0) peak. However, above $T \sim 20$ K, denoted by the dashed line in the figure, the temperature dependence of the superlattice peak is considerably different from that of the (7,0,0) peak. As seen in Fig. 7(b), a characteristic change also occurs in the temperature dependence of $\xi_{\rm ch}(a)$ and $\xi_{\rm ch}(b)$, where the correlation length suddenly extends. Furthermore, the incommensurability 2ε saturates into 0.24 below 20 K [see Fig. 7(c)]. These behaviors show that there is a characteristic temperature $T_{\rm lock}$ also in $x=0.09$, which is lower than that in $x=0.075$. At the lowest temperature, $\xi_{\rm ch}$ becomes almost isotropic but the correlation length remains ~80 Å, which is shorter than that in both $x=0.05$ and $x=0.075$. The result implies that the order parameter of the charge order for $x=0.09$ is reduced comparing with that for $x=0.05$ and $x=0.075$. As shown in Fig. 7(d), 2η is also temperature independent.

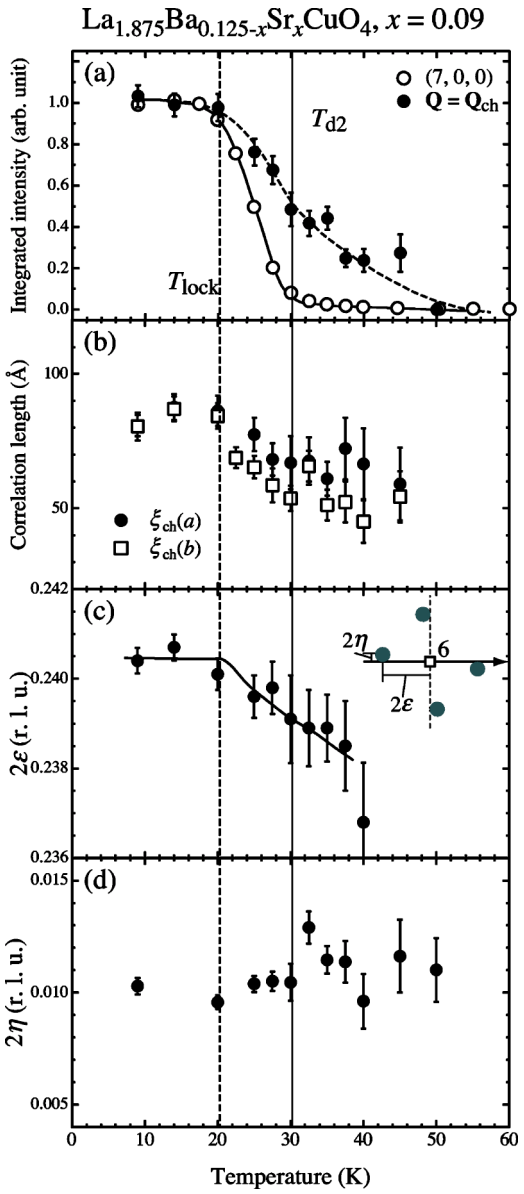

FIG. 7. Temperature dependences of (a) integrated intensity for the superlattice peak (closed circles) and the (7,0,0) peak (open circles), (b) correlation length along the *a* axis (closed circles) and *b* axis (open squares), (c) 2ε, (d) 2η for $x=0.09$. Definitions of 2ε and 2η are shown in the inset of (c). The bold and dashed curves are guides to the eye.

IV. DISCUSSION AND CONCLUSIONS

A. Modulation wave vector of a charge order

We first refer to the IC modulation wave vectors of the charge order. The present study confirmed that the modulation vector $q_{\rm ch}$ for $x=0.05$, $x=0.075$, and $x=0.09$ is $(0.239,0,1/2)$, $(0.236,-0.010,1/2)$, and $(0.240,-0.010,1/2)$, respectively.[13] Note that the concentration of (Ba+Sr) ions for the $x=0.075$ sample is roughly estimated to be 0.117 by ICP emission spectroscopy, which is nearly consistent with the $\varepsilon(=0.118)$ for $x=0.075$. Therefore, the effective concentration of doped holes almost coincides with the incommensurability of the modulation wave vector, which suggests a 1/4-filling configuration in the charge stripes.

$q_{\rm ch}$ for $x=0.075$ and $x=0.09$ shows that the IC modulation wave vector does not lie on the fundamental reciprocal axis (i.e., *H*, or *K* axis), which has been originally found in the IC magnetic order of La_2CuO_{4+y}.[14] This shift from the symmetry axis is quantified by the angle of θ_Y between the modulation wave vector and the *H* (or *K*) axis. The definition of θ_Y is displayed in Fig. 8(a). Fujita *et al.* have found[8] that the amplitude of θ_Y in the LBSCO system is proportional to the square value of the orthorhombic distortion ($\equiv\theta_{\rm ortho}$), which is quantified as the deviation from 90° in the angle between the *H* and *K* axis in the HTT unit [see Fig. 8(a)]. As shown in

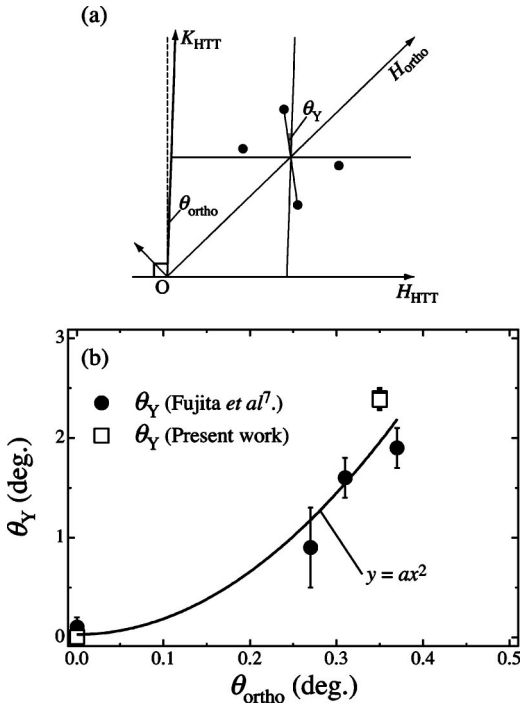

FIG. 8. (a) Schematic representation of the geometry of the IC magnetic peaks and the definitions of θ_{ortho} and θ_Y. (b) θ_Y as a function of θ_{ortho}. Closed circles and open squares were obtained by Fujita *et al.* (Ref. 7) and from the present study, respectively.

Fig. 8(b), θ_Y as a function of θ_{ortho} obtained by Fujita *et al.* (closed circles) agrees well with the results obtained in the present study (open squares). Note that θ_Y and θ_{ortho} for $x=0.075$ and $x=0.09$ almost coincide within the experimental error. Theoretical work based on *fermiology* has pointed out that θ_Y can be understood as an anisotropy of the second nearest-neighbor transfer integral due to the orthorhombic symmetry in the CuO_2 plane.[15] However, a detailed displacement pattern of oxygen atoms associated with the charge order should be resolved to explain the origin of the peak shift.

B. Order parameter of structural phase transitions and a charge order

Structural phase transitions from the LTO to LTLO, and from the LTO to LTT phase, in La-214 cuprates can be understood in terms of the Landau-Ginzburg free energy of the order parameter, which is described by the amplitude of the tilting of CuO_6 octahedra.[6,16] In this framework, the LTO-LTT transition shows a first-order phase transition while the LTO-LTLO transition should be a second-order phase transition, which depends on the sign of the eighth-order term in expanding the Landau free energy. Therefore, the structural phase transition in $x=0.05$ is a first order while $x=0.075$ and $x=0.09$ should show a second-order phase transition. X-ray powder diffraction analyses have shown that the LTO-LTT transition in $La_{1.875}Ba_{0.125}CuO_4$ is a first order transition, where both the LTO and LTT phases coexist and the volume fraction of the LTT phase increases with decreasing temperature.[6,17] Therefore, the temperature dependence of (5,0,0) intensity and ξ_b for $x=0.05$, shown in Figs. 5(a) and 5(b), can be regarded as the change of the volume fraction of LTO and LTT structure. Based on this argument, it is plausible that the difference between the temperature evolution near T_{d2} of the charge order for $x=0.05$ and that for $x=0.075$ and $x=0.09$ closely correlates with the order of each structural phase transition. In the case of $x=0.05$, there is no critical phenomenon associated with the charge order because the structural phase transition is a first order one. On the contrary, for $x=0.075$ and $x=0.09$, the short-range charge correlation above T_{d2} is induced by the successive increase in structural instabilities or fluctuations near the second-order LTO-LTLO phase transition. It should be noted that x-ray diffraction integrates over both elastic and inelastic scattering. Therefore there is also a possibility that the weak signals above T_{d2} indicate dynamical charge (stripe) correlations.

C. Correlation length

The coherence of the LTT structure for $x=0.05$ along the b axis (ξ_b) extends with decreasing temperature but remains within a finite length ($\sim$200 Å). In contrast, the coherence of the LTLO structure for $x=0.075$ and $x=0.09$ is almost long ranged. The correlation length of the charge order, however, is less than $\sim$100 Å for all the samples, which is much shorter than the structural coherence. These results show that the charge stripes in this system are essentially glassy or topologically disturbed. Comparing ξ_{ch} with the correlation length of the magnetic order ($\equiv\xi_{\mathrm{spin}}$) obtained by the previous neutron scattering study,[8] we thus obtain the ratio; $\xi_{\mathrm{spin}}/\xi_{\mathrm{ch}}>2$. Note that in LNSCO[18] and $La_{5/3}Sr_{1/3}NiO_4$,[19] $\xi_{\mathrm{spin}}/\xi_{\mathrm{ch}}$ is about 4 and 3, respectively. Zachar *et al.* have argued, from a theoretical standpoint, that in the case of $1<\xi_{\mathrm{spin}}/\xi_{\mathrm{ch}}\lesssim 4$, charge stripes are disordered by nontopological elastic deformations, resulting in a Bragg-glass-like state or a discommensuration.[20]

Charge correlation ξ_{ch} for $x=0.075$ and $x=0.09$ becomes longer below around T_{lock}, where the evolution of the superlattice peak is superposed with that of $(5,0,0)/(7,0,0)$ peaks and the IC modulation wave vector is locked. Based on the stripe model, $\xi_{\mathrm{ch}}(a)$ denotes the deformation of the periodicity or the discommensuration for charge stripes and $\xi_{\mathrm{ch}}(b)$ corresponds to the mosaicity of stripes. From this point of view, the results for $x=0.075$ and $x=0.09$ indicate that the deformation of the stripe periodicity and the stripe mosaicity are reduced as temperature decreases and 2ε is pinned finally at the value of hole concentration. If the $1/4$ filling is robust in the charge stripes, the temperature variation of 2ε indicates that the number of localized holes increases with decreasing temperature, which immobilizes charge stripes. The locking of the incommensurability is also seen in LNSCO[11] and striped nickelates.[21] However, the connection between the locking effect and the structural phase transition was not observed in either case. Note that the temperature dependence of the incommensurability for magnetic order should be compared with that of 2ε in the $x=0.075$ and $x=0.09$ samples to clarify the microscopic interrelation between the spin and charge correlations.

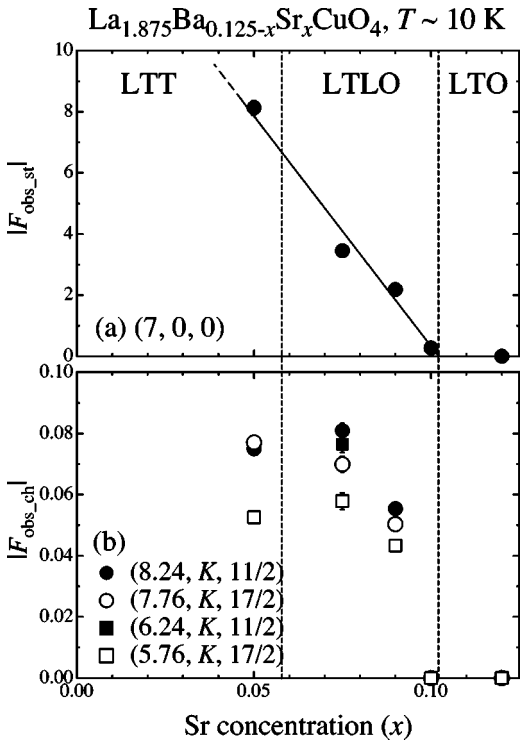

FIG. 9. Absolute value of the structure factor at ~10 K for (a) (7,0,0) peaks ($\equiv|F_{\mathrm{obs\_st}}|$) and (b) IC superlattice peaks ($\equiv|F_{\mathrm{obs\_ch}}|$) taken at four reciprocal lattice points as a function of Sr concentration. The results of Ba-free $x=0.12$ (LSCO $x=0.12$) are also shown (Ref. 22).

D. Comparison of structure factors

We finally compare quantitatively the structure factors of the lattice distortion associated with the charge order for $0.05\leqslant x\leqslant 0.10$.

The integrated intensity of the superlattice peaks were converted into the absolute value of the structure factor $|F_{\mathrm{obs\_ch}}|$ using the scale factor obtained from the measurements of fundamental Bragg intensities. The absolute value of the structure factor for the LTT/LTLO structure ($\equiv|F_{\mathrm{obs\_st}}|$) were also obtained to compare with each $|F_{\mathrm{obs\_ch}}|$. Figure 9 shows $|F_{\mathrm{obs\_st}}|$ and $|F_{\mathrm{obs\_ch}}|$ as a function of Sr concentration. The figure includes the result of Ba-free $x=0.12$ (LSCO $x=0.12$) taken previously.[22] As seen in Fig. 9(a), $|F_{\mathrm{obs\_st}}|$ linearly increases with decreasing Sr concentration. It shows that atomic displacements of La (Ba, Sr) and O associated with the LTT/LTLO structure increase as Sr concentration decreases. $|F_{\mathrm{obs\_ch}}|$ also shows the linear relation with Sr concentration in the LTLO phase. Thus we speculate that the charge order in the LTLO phase becomes more stable as a pinning potential in the CuO_2 plane increases, which is consistent with the fact that T_{lock} becomes higher as Sr concentration increases. However, $|F_{\mathrm{obs\_ch}}|$ of $x=0.05$ in the LTT phase is comparable with that of $x=0.075$ in the LTLO phase while $|F_{\mathrm{obs\_st}}|$ of $x=0.05$ is much stronger than that of $x=0.075$. The result implies that the structure factor of the lattice distortion associated with the charge order in the LTT structure is different with that in the LTLO phase; namely, the displacement pattern of oxygen atoms in the LTT phase is different from that in the LTLO phase.

E. Conclusions

The relationship between charge stripes and structural phase transitions was systematically studied for $La_{1.875}Ba_{0.125-x}Sr_xCuO_4$ with $0.05\leqslant x\leqslant 0.10$. We have found that the short-range charge correlations appear above T_{d2} for $x=0.075$ and $x=0.09$ while the correlation start growing just at T_{d2} for $x=0.05$. Furthermore in both the $x=0.075$ and $x=0.09$ samples, the temperature dependence of the correlation length and the incommensurability are different from those for the $x=0.05$ sample. These facts are closely related with the order of the structural phase transitions from the LTO phase to the LTLO or LTT phases. The quantitative comparison of the structure factors for the charge order and the LTT/LTLO structure reveals that the charge order becomes more robust as the order parameter of the LTLO structure increases. Comparison of $|F_{\mathrm{obs\_ch}}|$ for tetragonal $x=0.05$ with that for orthorhombic $x=0.075$ indicates that the displacement pattern induced by the charge order in the LTT phase is different from that in the LTLO phase. A detailed structure analysis in the charge ordered phase is required to discuss more quantitatively. The structure analysis for $x=0.05$ is now in progress. Thus the detailed displacement pattern induced by the charge order will be clarified in the near future.

ACKNOWLEDGMENTS

The authors thank M. Ito, K. Machida, H. Yamase, and O. Zacher for valuable discussions. This work was supported in part by a Grant-In-Aid for Young Scientists B (13740216 and 15740194), Scientific Research B (14340105), Scientific Research on Priority Areas (12046239), and Creative Scientific Research (13NP0201) from the Japanese Ministry of Education, Science, Sports and Culture, and by the Core Research for Evolutional Science and Technology (CREST) from the Japan Science and Technology Corporation. The synchrotron x-ray experiments were carried out at the SPring-8 facility (Proposal No. 2002A0314, R03A46XU, 2003B0117, and 2004A2117).

*Electronic mail: kimura@tagen.tohoku.ac.jp

[1] S. A. Kivelson, E. Fradokin, and V. J. Emery, Nature (London) **393**, 550 (1998).

[2] J. M. Tranquada, B. J. Sternlieb, J. D. Axe, Y. Nakamura, and S. Uchida, Nature (London) **375**, 561 (1995).

[3] J. M. Tranquada, J. D. Axe, N. Ichikawa, Y. Nakamura, S. Uchida, and B. Nachumi, Phys. Rev. B **54**, 7489 (1996).

[4] J. M. Tranquada, J. D. Axe, N. Ichikawa, A. R. Moodenbaugh, Y.

Nakamura, and S. Uchida, Phys. Rev. Lett. **78**, 338 (1997).
[5] A. R. Moodenbaugh, Y. Xu, M. Suenaga, T. J. Follcerts, and R. N. Shelton, Phys. Rev. B **38**, 4596 (1988).
[6] J. D. Axe, A. H. Moudden, D. Hohlwein, D. E. Cox, K. M. Mohanty, A. R. Moodenbaugh, and Y. Xu, Phys. Rev. Lett. **62**, 2751 (1989).
[7] M. Fujita, H. Goka, K. Yamada, and M. Matsuda, Phys. Rev. Lett. **88**, 167008 (2002).
[8] M. Fujita, H. Goka, K. Yamada, and M. Matsuda, Phys. Rev. B **66**, 184503 (2002).
[9] H. Kimura, H. Goka, M. Fujita, Y. Noda, K. Yamada, and N. Ikeda, Phys. Rev. B **67**, 140503 (2003).
[10] H. Kimura (unpublished).
[11] M. V. Zimmermann, A. Vigliante, T. Niemöller, N. Ichikawa, T. Frello, J. Madsen, P. Wochner, S. Uchida, N. H. Andersen, J. M. Tranquada, D. Gibbs, and J. R. Schneider, Europhys. Lett. **41**, 629 (1998).
[12] Y. Noda, K. Ohshima, H. Toraya, K. Tanaka, H. Terauchi, H. Maeta, and H. Konishi, J. Synchrotron Radiat. **5**, 485 (1998).
[13] The q_{ch} for $x=0.075$ has been obtained as $(0.24-0.007\,1/2)$ at the previous experiment (Ref. 9). However, the result of the present study is more reliable because the instrument resolutions and the statistics are much more improved than those of the previous work.
[14] Y. S. Lee, R. J. Birgeneau, M. A. Kastner, Y. Endoh, S. Wakimoto, K. Yamada, R. W. Erwin, S.-H. Lee, and G. Shirane, Phys. Rev. B **60**, 3643 (1999).
[15] H. Yamase and H. Kohno, J. Phys. Soc. Jpn. **69**, 332 (2000).
[16] W. Ting, K. Fossheim, and T. Lægreid, Solid State Commun. **75**, 727 (1990).
[17] S. J. L. Billinge, G. H. Kwei, A. C. Lawson, and J. D. Thompson, Phys. Rev. Lett. **71**, 1903 (1993).
[18] J. M. Tranquada, N. Ichikawa, and S. Uchida, Phys. Rev. B **59**, 14 712 (1999).
[19] S.-H. Lee, S. W. Cheong, K. Yamada, and C. F. Majkrzak, Phys. Rev. B **63**, 060405 (2001).
[20] O. Zachar, Phys. Rev. B **62**, 13 836 (2000).
[21] R. Kajimoto, T. Takeshita, H. Yoshizawa, T. Tanabe, T. Katsufuji, and Y. Tokura, Phys. Rev. B **64**, 144432 (2000).
[22] H. Kimura (unpublished).